Chapter V

Application to a Fusion Problem

A. Introduction

The series of calculations discussed in this chapter was done in support of a newly proposed Magnetized Target Fusion (MTF) concept (Thio, C. F. et al., 1998 [84], [85]) and the results were presented at the 1998 Innovative Confinement Concepts Workshop, at Princeton, NJ, April 6-9, and at ICOPS '98, Raleigh, NC. The results presented at ICOPS '98 were done with the explicit code. In the present discussion some comparison of the implicit and explicit code is presented.

It was hoped that the implicit code could be shown to model parts of the computations of a practical problem faster than the explicit code. This has not happened yet, but this application has demonstrated that the two codes are in good agreement in 2D and 3D. A regime where the implicit code has functioned faster than the explicit code was discussed in Chapter IV, Section G, but it came too late for this ability to be expanded into a practical problem. The regime was found after this dissertation was essentially written.

The new MTF concept consists of sixty or more neutral plasma jets in a spherical arrangement, imploding one or two small magnetized toroidal plasma targets. The plasma jets and targets are to consist of deuterium and tritium (D -T), and since they are in a neutral plasma state, they can be approximately modeled using hydrodynamic methods. The jets, as envisioned, will merge together and form a spherically imploding piston or liner. Once the target ignites, the liner will supply fuel for the imploded target to burn. The jets are accelerated from plasma guns by a heavier ionized gas, possibly argon. The

heavier argon would also act as a tamper during implosion, and an absorber for x-rays to help protect the chamber and plasma guns from x-ray damage. Another layer of plasma could be introduced behind the argon, such as lithium or boron to absorb neutrons.

Each target can be thought of as the plasma equivalent of a smoke ring confined by a stable toroidal magnetic field. It is well understood how to produce the plasma rings from specially designed plasma guns, and the toroidal configuration of the magnetic field in the targets is known to be stable [89]. The magnetic pressures will be weak compared to the hydrodynamic forces; hence, for the present calculations the target is replaced with a sphere or cylinder of neutral gases, and the magnetic field is ignored.

It was hoped that the implicit code would be able to perform the calculations up to the time of impact of the jets with the target including the merging of the jets. This, however, has not been demonstrated yet. The implicit code has been run on all three cases discussed in this chapter.

Magnetized Target Fusion is a cross between Magnetic Fusion Energy (MFE), which uses a magnetically confined D-T plasma (for example the Tokamak), and Inertially Confined Fusion (ICF), in which a D-T target is imploded by laser or particle beams. MTF starts with a magnetized target and implodes it with any one of a number of means. The magnetized target is the important difference, because the magnetic fields of the target confine the ions and electrons, reducing the loss of energy from the target. It has been shown that such a target does not need as large a driver to initiate fusion as ICF requires [42], [50], [74]. The targets will be much larger and will require a less energetic driver.

The explicit SPHINX code was used for all of these calculations, and a few of the

simpler calculations were repeated with the implicit code. The calculations are preliminary and address only the hydrodynamic aspects of the problem. The study was mainly concerned with the merger of the jets and the formation of the imploding piston. Fusion was not considered in detail, except that the temperatures and confinement durations for ignition were sought within a few attempts, but no optimization was performed.

The following assumptions were made for these calculations. The D -T plasma jets are considered neutral, so that no magnetic or electric fields are present. Losses due to radiation and thermal convection were not included. It is assumed that radiation losses will be insignificant up to the time of maximum compression. The argon driver plasma might not be neutral, so it might have electric and magnetic fields in it, and hence was not modeled in the present set of calculations.

The first set of calculations considered a simple case of two jets merging at an angle and then accelerating a solid aluminum projectile. The next set of problems consisted of a cylindrical ring of jets aimed at the origin and a target of D -T. The third set of calculations modeled the 3D spherical arrangement of jets, and consisted of 60 jets in a soccer ball configuration, similar to the target chamber of the Omega laser fusion system at the University of Rochester, N.Y.. A soccer ball is covered with an arrangement of hexagons and pentagons, and the jets were placed at each of the sixty vertices.

B. Neutral Plasma Jets Merging onto a Projectile

The goals of this first set of calculations were (1) to see how the neutral plasma jets merge together, and (2) to find to what maximum velocity a small projectile can be acceler-

ated using plasma jets of different masses and velocities. The momentum was varied but not the energy, to see if this affected the coupling of the energy into the target. The acceleration of projectiles to high velocities is of interest to the weapons community. The gas for the jets in this case is not D -T but a more massive gas. The problem was done with two jets, in 2D, using the explicit and implicit codes. The initial setup is shown in Fig. V. 1.

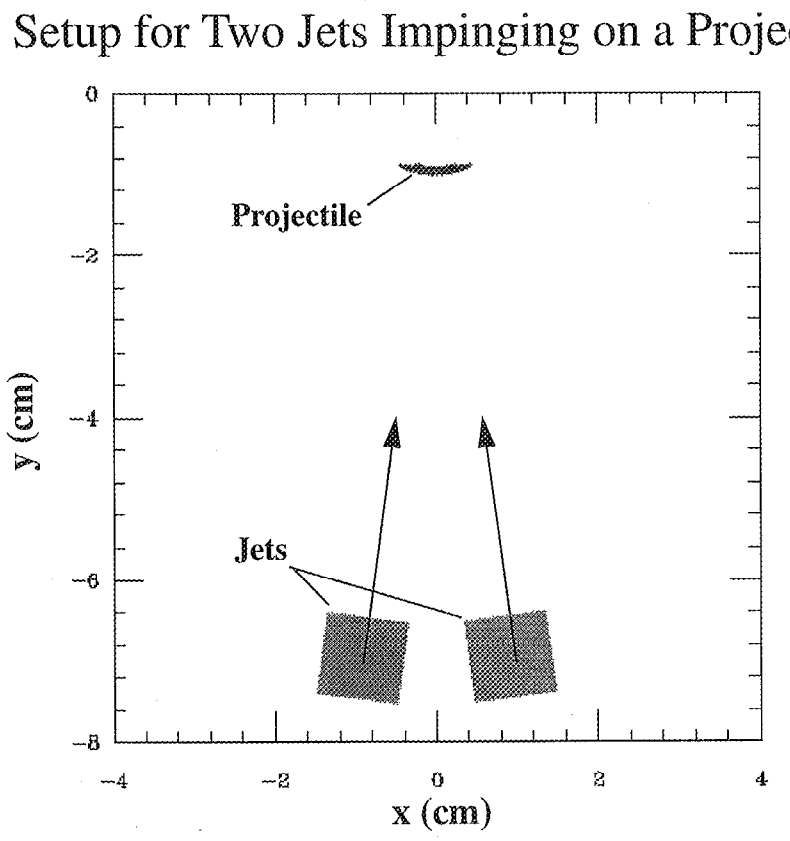

Fig. V. 1. This is the initial setup for two plasma jets impinging on an aluminum projectile. The jets are aimed at the origin, and the target is placed ahead of the origin.

The initial setup consisted of two jets, 15 degrees apart, and aimed at the origin, which was behind a stationary aluminum projectile. As the jets move toward the projectile, they expand due to internal pressure. On the way to the projectile, the jets collide with each other, forming a more dense core between them, and the squeezing of the core

produces what will be referred to here as a "super-jet", where the particles at the leading edge of the core are accelerated forward toward the origin and those at the rear of the core are accelerated backward. In some cases the super-jets were found to cut the projectile into pieces. This problem can be lessened by starting the jets farther away from the projectile thus allowing the super-jet to spread out before striking the target.

The velocities v and masses m of the jets were varied so as to increase the momentum but maintain constant energy between case studies. If the mass of the jets is increased by a factor of four and the velocity decreased by a factor of two, the momentum (mv) will be doubled while the energy $1/2(mv^2)$ is kept constant between cases. The question then is: can the energy of the jets be transferred more efficiently to the target by increasing the momentum of the jets while maintaining constant energy?

Three cases were run: (1) with the density of the jets set to 0.006 gm/cc, and a bulk velocity of 100 km/sec, (2) with a density of 0.024 gm/cc and a velocity of 50 km/sec, and (3) with a density of 0.096 gm/cc and a velocity of 25 km/sec. The jets were modeled as a perfect gas with $\gamma = 1.4$, the ratio of specific heats, and $\mu = 1$, the average molecular weight. The initial temperature of the jets was set to 11,600 degrees Kelvin (1 ev). Each jet was represented by a 1x1 cm square rectangle of particles. There were 900 particles in each jet and 66 in the projectile. The projectile was aluminum using a linear_u_s_u_p material-strength model, and the input for aluminum included: a solid density of 2.7 gm/cc, a sound speed of $c_o = 5.376e5$ cm/sec, a slope of $s = 1.55$, $\gamma_0 = 2.1$, and $\gamma_1 = 0.0$.

Preliminary computer runs showed that the distance from the leading edge of the jets to the projectile should be about 7 to 5 cm, so that there was not too much overall

expansion in transit, and the super-jets had a chance to spread out. It was necessary to shorten the distance for the runs with slower velocities, so that they would all have about the same transit time; otherwise the expansion would become too great.

An inward velocity can be added to each particle in a jet, as a function of its distance from the axis of the jet, to counter the expansion due to the internal pressure, which would approximately model the inward focusing that a slight taper inside the plasma gun might impart to the jet. It was found by trial and error that the best range of focusing velocities was for the inward component of the velocity at the edge of the jet to be an order of magnitude less than the bulk velocity. This feature was used only in this two-jet problem, where the emphasis was on getting the most particles to strike the projectile. It was not used in the implosion calculations because there the jets will confine each other.

The first case, with the density of 0.006 gm/cc and the velocities of 100 km/sec, was set up with the Al projectile positioned −1.0 cm from the origin and the leading edge of the jet started at a position of −6.5 cm from the origin, so that the jets were located 5.5 cm from the projectile. A focusing velocity, of 10 km/sec, was added to the jets.

The jets first started to merge when they were about 3.4 cm from the projectile at time t = 0.202 μsec, and the pressure, temperature, and density between the jets began to increase. The two jets formed a butterfly shaped pattern (see Fig. V.2) with a denser core between the jets and less dense wings out to the sides. Then at time t = 0.460 μsec the jets first impacted the projectile. At the time of impact the wing pattern was about the same width as the projectile, so that most of the jet particles contributed to the impact. The final velocity of the projectile was about 5.9 km/sec as obtained with the explicit code.

Comparison of the Implicit and Explicit Codes at t = 4.5 μsec, for Two Jets Merging

(a)

(b)

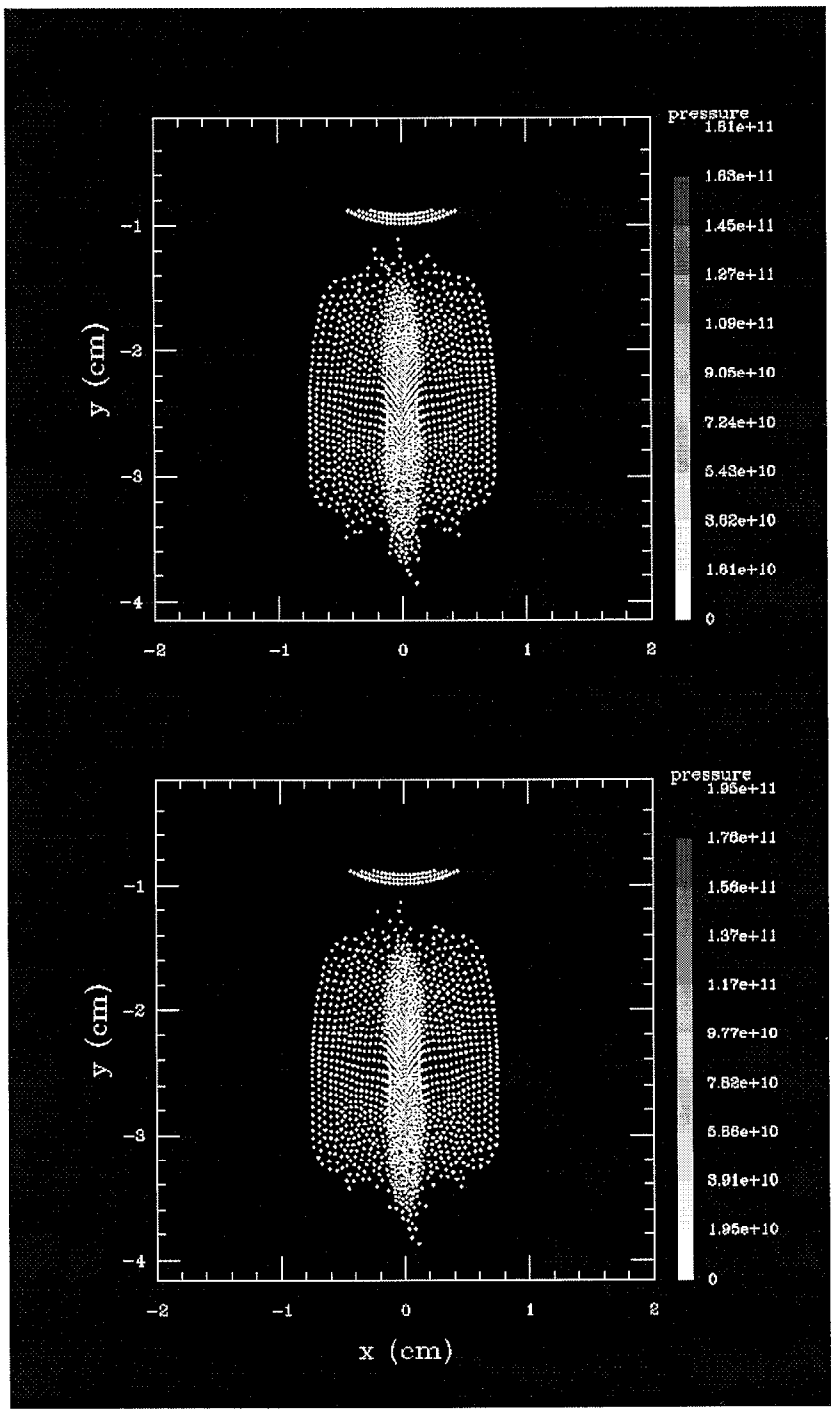

Fig. V. 2 This is a comparison of the implicit (a) and explicit (b) codes for two merged jets at 4.5436 and 4.5227 μsec respectively. Both codes had 1866 particles. An overlay of the two plots shows that the particle positions, in general, are in very good agreement.

This case was also run using the implicit code. An overlay of the two plots of Fig. V. 2 would show that the particle positions are in very good agreement except for a few particles at the leading and trailing edges. Unfortunately the implicit code stopped running at the point of impact, so there is no comparison for the projectile motions.

The jets were initially displaced relative to each other in the y-direction by half a smoothing length, which is why the results are not exactly symmetric. This small displacement was made to see if there would be a mixing of particles. If they were left completely symmetrical, one jet would be the mirror of the other, and there would be no mixing. Even with the offset there was very little mixing except within the super-jets.

The second case, with the density of 0.024 gm/cc, was set up with the projectile positioned as before, but the jets were set only 5.0 cm from the projectile, to accommodate the slower velocities. Since the jet velocities were reduced by a factor of two, to 50 km/sec, the focusing velocities had to be reduced by the same factor of two so that they were still an order of magnitude less than the jet velocities.

The jets first interacted at about $t = 0.15$ μsec when they were about 5.2 cm from the projectile. At about $t = 0.7$ μsec the jets impacted the projectile. At the time of impact the denser core between the jets had expanded to engulf the wings, but the width of the jets was about the same as the projectile, so that again most of the particles contributed to the impact. The projectile was separated into several chunks and several individual particles. The final velocities ranged from 3.7 to 7.9 km/sec for the individual particles whereas the main chunks had velocities of 5.3, 5.9, and 7.1 km/sec.

The third case, with the density of 0.096 gm/cc and a velocity of 25 km/sec, was

set up with the projectile also at −1.0 cm from the origin, and a 5.0 cm separation between the jets and the projectile. For this case the jets were moving too slowly for the focusing to be of any use, because the reduced focusing velocity in x was quickly overwhelmed by the pressure within expanding jets. The wings expanded too fast to be of much use, so the distance was chosen to adjust the core width to fit the projectile.

The jets started to interact at about 0.25 μsec at a distance of about 5.2 cm from the projectile. For this case the core had expanded to a little more than the width of the projectile and the wings had expanded quite a bit more so that they missed the projectile. In this case, approximately half of the particles hit the projectile, so the momentum was inefficiently transferred to the projectile. The projectile was cut in two, and a few individual particles were scattered around. The velocity of the bulk of the particles was roughly 4.5 km/sec. Variations on this case could be tried in which the focusing velocity could be increased or the distance between the jets and the projectile could be decreased.

Drawing a conclusion from this, it appears that there are other aspects to consider when trying to go to higher momentums. The higher momentums seem to cut the projectile up. Also the slower velocities allow the jets to expand more in transit to the projectile making it more difficult to get all of each jet to hit the projectile, and an added focusing velocity has less effect on keeping the jet together because it is more quickly overwhelmed by the pressure. It appears that the high velocity of the lower momentum case helped more by getting the jets to the projectile before they had a chance to expand. So there is a trade off between the higher velocities and the higher momentum and distances.

C. The 2D Ring of Jets

This set of calculations was performed to learn how uniform an imploding plasma piston ring can be made and how long it can confine the target particles. It was also learned what densities and temperatures could be achieved, from a hydrodynamic standpoint, for the implosion of a given target. The initial setup is shown in Fig. V. 3.

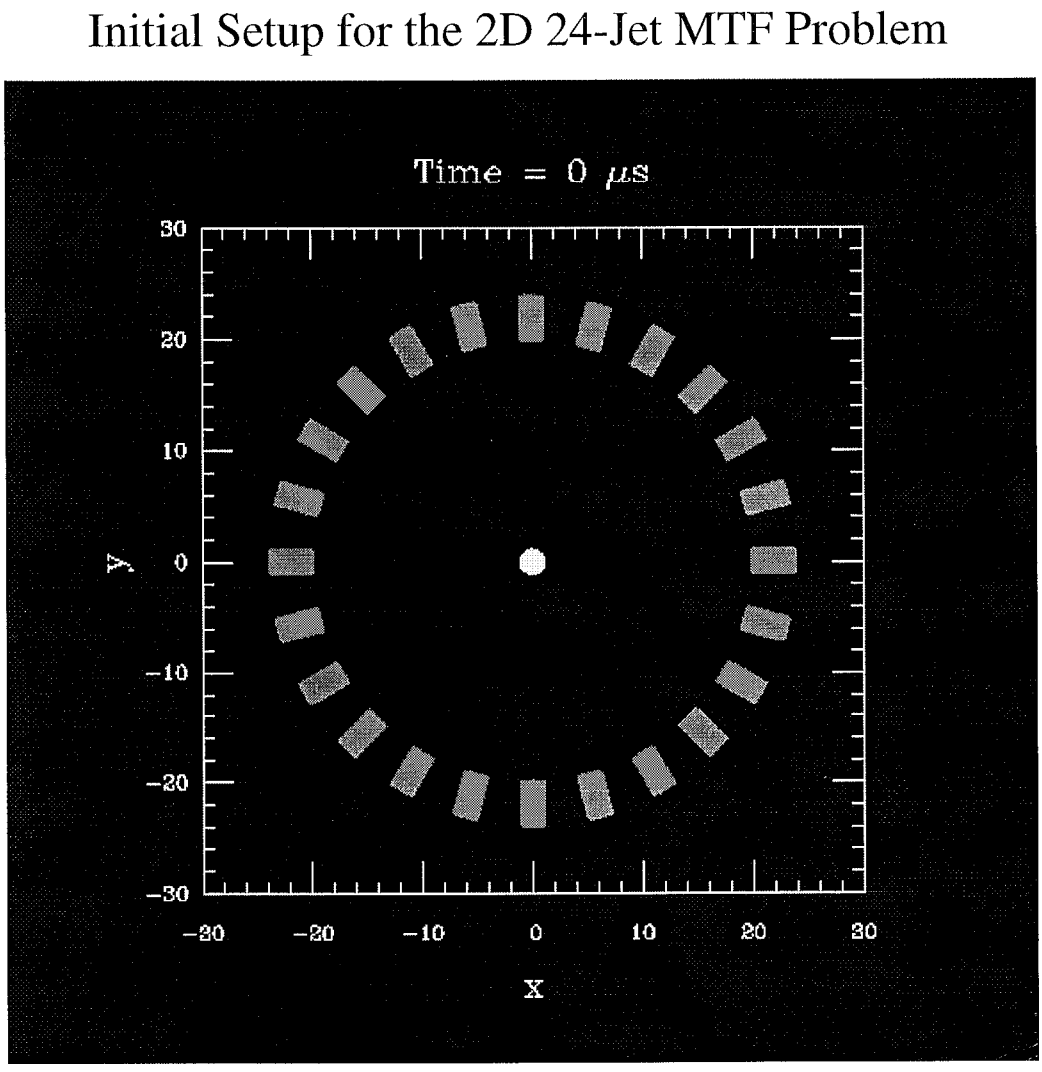

Fig. V. 3. This is the initial setup for the 24-jet case in 2D. The jets are about 20 cm from the target. Only one quadrant was calculated and then reflected around into the other three quadrants.

These calculations were done in 2D, and considered 24 jets in a ring positioned at every 15 degrees, and 20 cm from the origin. Each jet was 1 cm in radius and 3.8 cm in length The jets are assumed to exit the plasma guns at an initial velocity of $5x10^7$ cm/sec with a density of 10^{-5} gm/cc, and all aimed at the origin. They were each given an initial temperature of 11,600 ^oK (or 1 ev). The target was modeled as a cylinder of radius 1cm, and given an initial temperature of 23,200 ^oK. The case discussed here used the perfect gas EOS. The total number of particles used was 12,322, with 2,016 per jet, and 226 in the quarter target for runs using the explicit code.

Because of the symmetry of the problem, only one quadrant of the problem was run with reflecting boundaries along the x- and y-axes. Taking advantage of the symmetry allows one to save on memory and computational time or to increase the resolution.

When the jets start merging with each other, they form the super-jets as discussed in the previous section on two-jets. An earlier attempt had only 12 jets positioned at every 30 degrees and closer to the target, but that did not allow the super-jets to spread out into a uniform front before hitting the target, and the super-jets tended to cut the target up. So the jets were moved back to 20 cm from the target and the number of jets increased to 24. This arrangement allowed the super-jets to merge farther away from the target and form a more uniform front by the time they reached the target.

Figure V. 4 shows the system at maximum compression. The initial contact of the super-jets with the target caused some fluting on the target surface. But the growth of the fluting ceased when the main part of the jets arrived, and then all the target particles were swept up and compressed. The fluting caused the filigree pattern around the compressed

target in Fig. V. 4. The jets have merged together to form an imploding cylindrical piston (this is also referred to as a liner in some literature) that is the uniform circular region around the target. The bulk of the jet particles are still streaming in and are stagnating in the piston, which is confining the target. Each particle of Fig. V. 4 has a velocity vector attached to it, hence the radial lines on the jet particles that are still imploding.

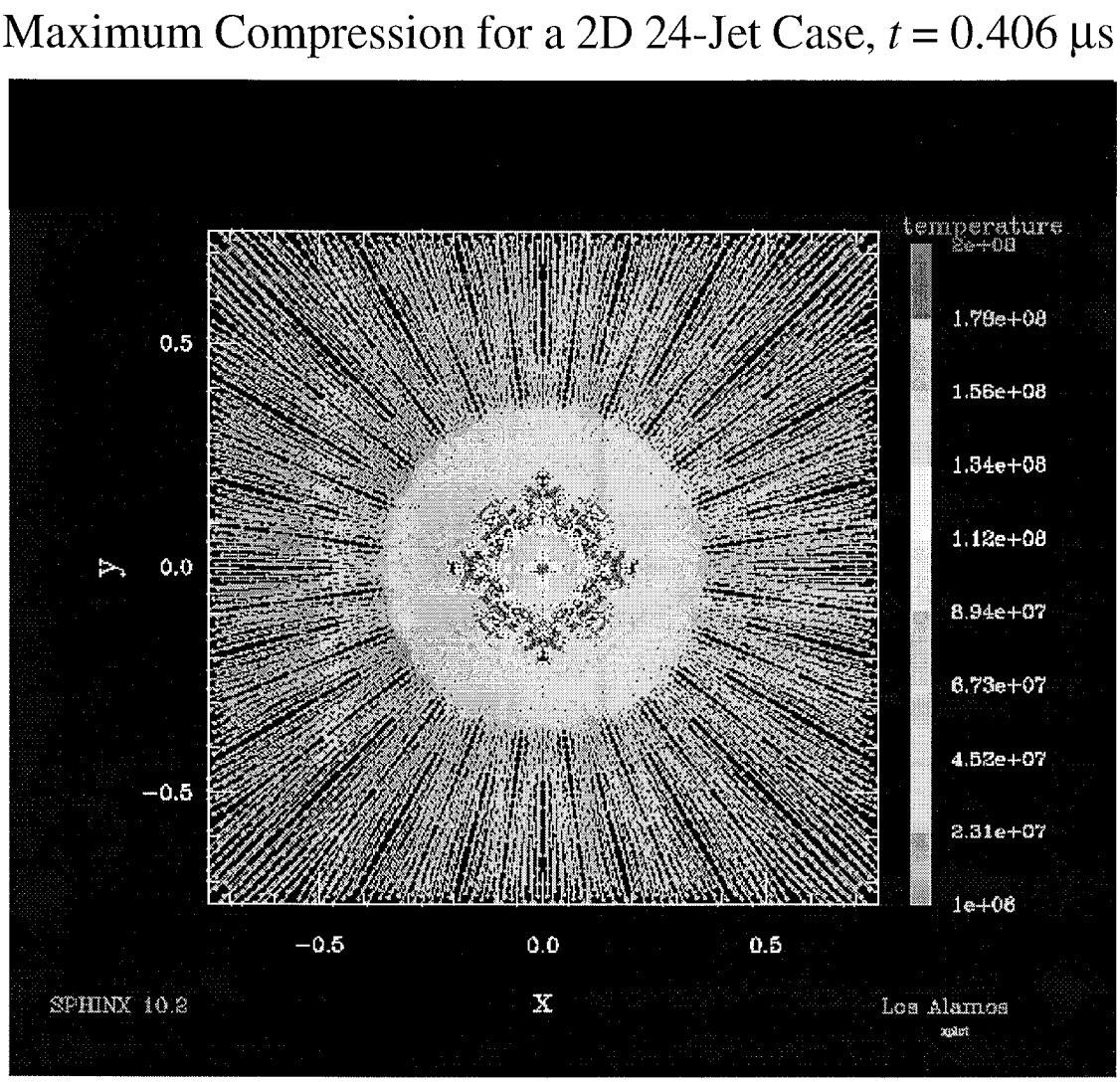

Fig. V. 4. This figure shows the 24-jet case at maximum compression. The target is the irregularly shaped pattern in the middle, of radius ~0.3 cm. The piston is forming around the target uniformly and is the circular region around it. The jets are still streaming in and have a velocity vector attached to each particle, hence the radial rays.

The uniformity of density and shape of the piston met expectations. Most of the particles in the piston, from time $t = 0.4$ μsec to $t = 0.45$ μsec, fall within a density range of 0.0002 gm/cc and 0.002 gm/cc. The pressure for most of the piston particles is in a range of about 2e11 to 2e12 dynes/cm The temperature was within a range of 6e6 to 5e7 ^{o}K. The trailing edge of the jets impacted the piston at about $t = 0.45$ μsec.

The target diameter, except for a few target particles, reached a minimum at $t =$ 0.406 μsec with a diameter of about 0.3 cm, stayed there until about $t = 0.45$ μsec, and was under 0.4cm until about 0.47 μsec. At this point it started to expand more rapidly but was still within a diameter of 0.6cm at $t = 0.5$ μsec. The duration of tight confinement of the target was about 70 nsec. The target material was compressed by a factor of about 37 times. Most of the target particles fell within a temperature band of 6e7 to 2e8 ^{o}K, and the pressure was between about 5e11 to 1.1e12 dynes/cm^2 during maximum compression.

The following results were obtained from a calculation around the maximum compression of the target.

Piston particles:		
Max temperature	T = 1.18e8 ^{o}K	at $t = 0.408009$ μsec.
Max pressure	P = 1.07e13	at $t = 0.412022$ μsec.
Max density	D = 0.00589 gm/cc	at $t = 0.412022$ μsec.
Target particles:		
Max temperature	T = 3.15e8 ^{o}K	at $t = 0.408009$ μsec.
Max pressure	P = 2.02e12	at $t = 0.408009$ μsec.
Max density	D = 0.000502 gm/cc	at $t = 0.406022$ μsec.

A few implicit runs were made repeating the explicit case discussed above to see how the implicit code would compare. It was hoped that the implicit code could compute

the early portion of the problem where the jets are running in and merging. However, the explicit code does this portion so quickly that it is difficult to beat it. The implicit code was run with 1,101 particles, 180 per jet, and 21 in the quarter target. It was run to a point close to where the particles first contacted the target. The implicit code's best wall clock time was about 28 minutes, whereas the explicit code took about a minute. An overlay of the results shows that agreement between the two codes is very good. If the implicit code is run through maximum compression of the target, it runs best at about the same time-step size as the explicit code. Both codes compress the target to about the same size and they both produce about the same size piston.

D. The 3D Sphere of 60 jets

For the 3D case, 60 D -T neutral-plasma jets, placed in a soccer ball arrangement of hexagons and pentagons, were all aimed at the origin, where a spherical D -T target was positioned (see Fig. V.5). The jets then formed a spherically imploding piston. The sides of the pentagons and hexagons are all equal length, and the distances from all vertices to the origin are equal. Therefore the angle between any two adjacent jets, on one edge of either a pentagon or hexagon, are all equal, because they all form equal triangles with the origin. However, the angle between the two jets across a pentagon or hexagon is different. Therefore, once the jets have merged, looking along a normal to the center of a pentagon or hexagon toward the origin, one will see a decrease in density of the spherical piston, as opposed to looking radially through one of the vertices. This, however, does not appear to affect the confinement of the target significantly for the duration of maximum implosion.

The Initial Setup for the 3D 60-Jet MTF Concept

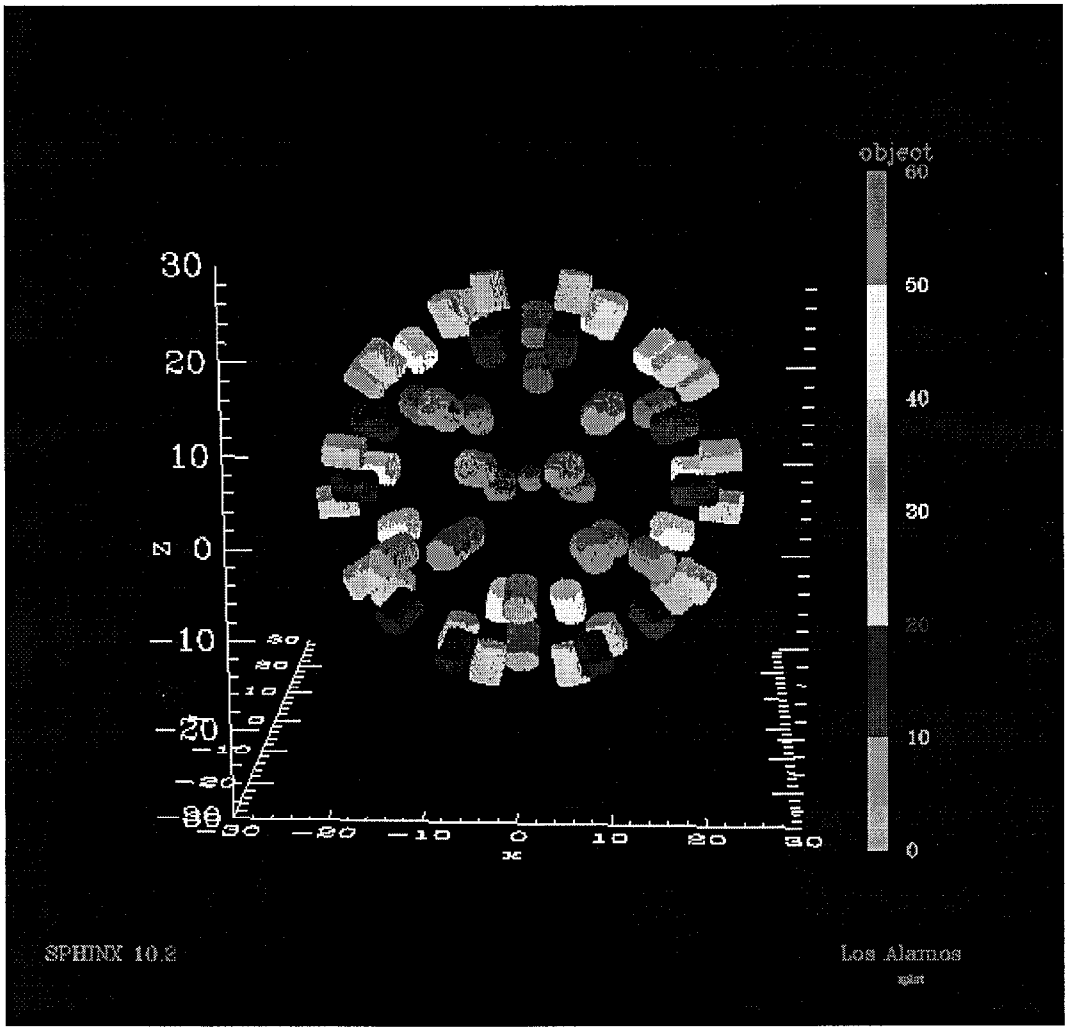

Fig. V. 5. The 60 cylindrical jets are arranged in a soccer ball pattern about a spherical target in the center. The jets are shaded according to their object number to help them show up against each other.

Initially the jets were made the same size as that used in the 24-jet case, 1cm in radius, but they started interacting only after they got fairly close to the target. So the jets were made wider, 1.5 cm in radius, so that they would start to interact farther away from the target. The super-jetting would, therefore, have time to spread out before striking the target. In three dimensions, the super-jets became sheets, interacting at different angles.

The sheets formed perpendicular to the sides of the hexagons and pentagons. The sheets interacted when they reached the center of a pentagon or a hexagon.

The total number of particles was 43,368, with 720 in each jet, and 168 in the target, using the explicit SPHINX code. All jets were modeled, i.e., no reflecting boundaries were used. The vertex positions were taken from a table generated for the Omega laser fusion target chamber. There is a plane of symmetry, but it does not coincide with either the x-y, x-z, or y-z plane. Since time was limited, it was simpler just to model all 60 jets rather than rotate all the vertex positions to an appropriate position to make the plane of symmetry coincide with one of the principal planes.

The initial conditions for the 60 cylindrical jets and a spherical target are specified in the following:

3D Case, 60-Jet Soccer Ball Pattern Imploding a Target Initial Conditions

(43,368 particles total: explicit code)
(5,768 particles total: implicit code)

D -T Jets

60 Jets in a soccer ball pattern, 20 cm from the Target.

Temperature:	11600 ^{o}K (1 ev).
Density:	2.0e–5 gm/cc.
Velocity:	5.0e7 cm/sec.
Dimension:	Cylinder, 1.7cm radius x 3.8cm length.
EOS:	Perfect Gas.

D -T Target

Temperature:	23200 ^{o}K (2 ev).
Density:	1.5e–5 gm/cc.
Dimension:	Sphere, 2.5 cm radius.
EOS:	Perfect Gas.

The results of the explicit code at $t = 0.4$ μsec are illustrated in Fig. V. 6. The par-

ticles shown in the figure are near maximum compression, however, only jet particles in a slab 0.25 cm on either side of the y-z plane are shown. The target particles have been removed from the plot to help illustrate the formation of the piston. The jets are coming from various angles, so the slab takes a slice through only a few of the jets and at different angles.

Maximum Compression for the 3D 60-Jet Case, $t = 0.4$ μs

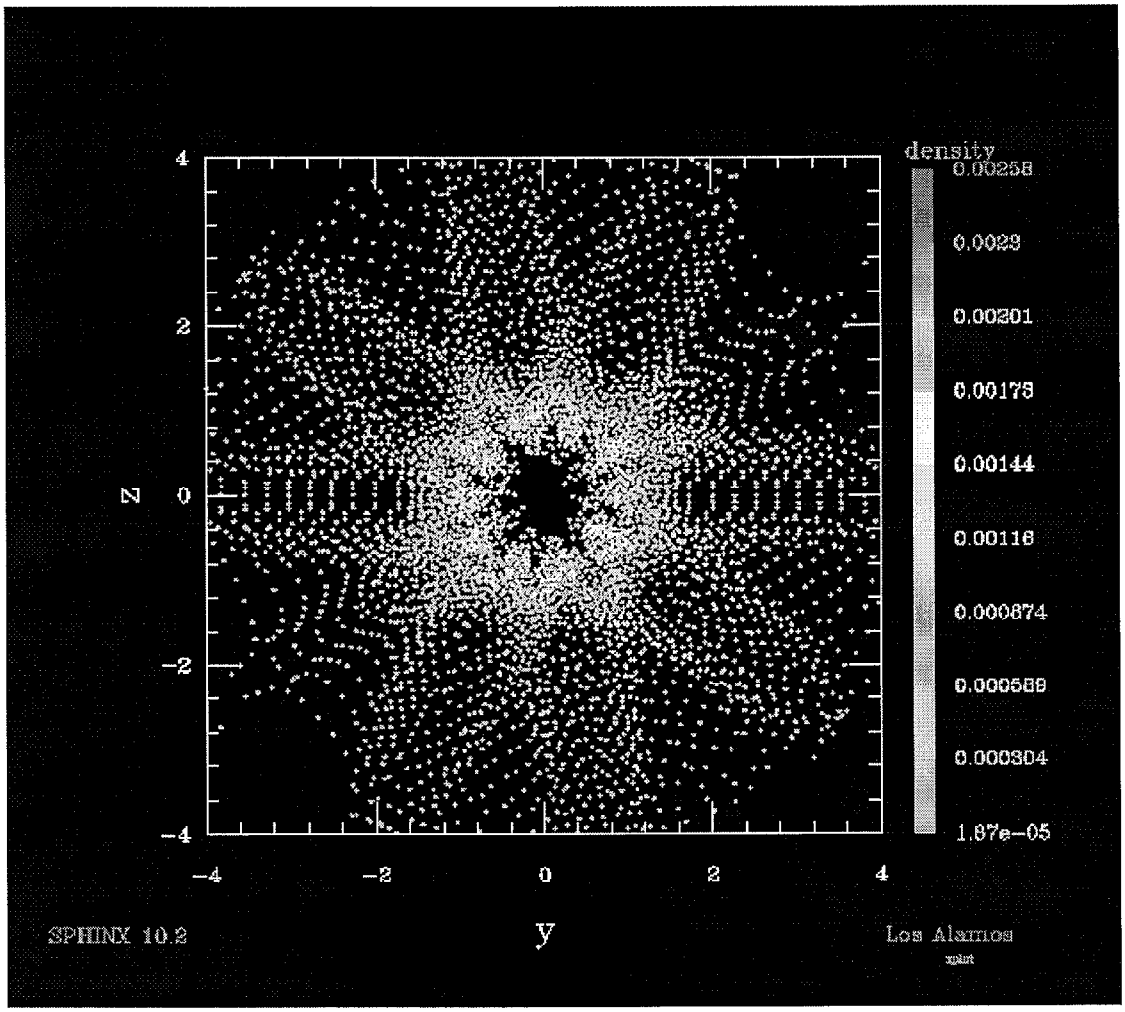

Fig. V. 6. This figure shows only jet particles from a 0.5 cm thick slab. The target particles have been removed to show the formation of the piston more clearly.

At maximum compression the target was heated to a temperature of 4.2×10^8 °K, and

compressed to a peak density of 0.0002 gm/cc and an average density of 0.00013 gm/cc for a duration of about 50 nsec. The piston reached an average density of 0.00065 gm/cc for a duration of about 70 nsec, and a peak density of 0.0023 gm/cc. The results are summarized in Table V. 1.

The following table shows a comparison of the 2D 24-jet case, the 3D 60-jet case, and the desired results.

Table 1: Comparison, at Maximum Compression, of SPHINX Calculations vs. Desired, t=0.4 μs.

	Desired	2D, 24 jets	3D, 60 jets
Target			
Temperature	10 kev	10 kev	10 kev
Density	0.001 gm/cc	0.0003 gm/cc	0.0005 gm/cc
Confinement	100 nsec	50 nsec	50 nsec
Diameter	1.0 cm	0.3 cm	1.2 cm
Piston			
Temperature	–	2.4 kev	3.0 kev
Density	–	0.002 gm/cc	0.0006 gm/cc
Confinement	100 nsec	70 nsec	70 nsec

This 3D problem was tried using the implicit code with the number of particles significantly reduced. There were a total of 5,768 particles, with 96 per jet, and 8 in the target. This case did run for a few time-steps, and all 60 jets were propagated toward the target properly, but before the jets started to interact, the allocation for memory was exceeded. The allocation could have been increased, but it was apparent that the implicit code was not going to do the problem any faster than the explicit code. However, this run

did demonstrate that the 3D aspects of the implicit code are working correctly, and it was able to handle nearly 6,000 particles.

E. Conclusions of the MTF study

The results of this study have shown that a fairly uniform spherical piston can be formed from an array of neutral plasma jets that start merging from some distance out from the target. When the jets first encounter each other, "super-jets" squirt out from between them. By varying the distance from the target, the super-jets are allowed to spread out and form a more uniform front before impacting the target. If the super-jets form too close to the target, they are found to cut up the target and not compress it as uniformly as desired.

Since this work has shown that a spherical piston might be formed from neutral plasma jets, and that conditions near D-T fusion can be reached, it would be very interesting to pursue this with an optimization study. One would want to look at varying the initial conditions such as the distance between the target and the jets; the densities, temperatures, and dimensions of the jets and the target; and the velocities and number of jets. Additional physics could be included in the explicit code, such as radiation losses and magneto-hydrodynamic capabilities.

Chapter VI

Conclusions

An implicit Smooth Particle Hydrodynamic code has been written, and has been demonstrated to give good agreement with analytic solutions, the explicit code, and experimental data for the various test cases tried. It has recently been demonstrated that for one case it can perform the calculations faster than the explicit code with Courant numbers of over 3,000, albeit a very unphysical problem (see Chapter IV, section G). This one case, however, does prove that it can be done, and it is a first step in expanding the code's capabilities to practical problems. In another case the code handled nearly 6,000 particles

This study is probing the boundaries of a new aspect of the field of SPH, and hence it may or may not be found to be a useful region for SPH to operate. The existing SPHINX code is typically used for high-velocity impact studies. An implicit code is best used for low-velocity, incompressible fluid problems. The new implicit code will need some changes to improve on the explicit code, but further work may yet make it useful for SPH.

The capabilities of the new implicit code, which is 1D, 2D, or 3D, include a choice of three Krylov solvers along with a multi-pass Jacobi preconditioner to solve the linear system. It also uses Newton-Raphson iteration methods with a line-search to solve the nonlinear problem.

The code uses sparse storage and sparse computations to minimize the amount of memory and time used. It also makes use of a new right-hand-side function in the SPHINX code, written just for these sparse matrices. Also, the Jacobian matrix is calcu-

lated numerically, as opposed to analytically, which allows the new code to take advantage of almost all of the existing physics that is already in the SPHINX code.

Five distinctly different versions of the code exist, and each newer version has shown a marked improvement in performance over the older ones. The first one uses LU Decomposition, a fourth-order Rosenbrock solver, and analytic derivatives for the Jacobian matrix, and stores the full matrix. It was very slow and cumbersome to use. The next version uses numerical derivatives, Krylov solvers, and Newton-Raphson iterations, but still calculates and stores the full Jacobian matrix. As a result it uses large amounts of memory, and performs many unnecessary calculations of zero. However, because of this factor it does catch some unexpected matrix elements that the summation density method generates. The sparse versions of the code will need to be modified to handle the summation method and are currently restricted to using the continuity equation.

The two sparse versions of the code are very similar, and both store only the non-zero elements of the Jacobian and do not calculate the portions of the matrix that are known to be zero, that is, the portions where there is no neighbor relation between particles. The difference is in the right-hand-side function, the function that calculates the time derivatives for each equation. One uses a function that calculates the rhs for all the particles, and the other uses a function that calculates the rhs for only one particle at a time. The latter one saves on calculations because for each particle the rhs function only has to be calculated for its neighbors, not all particles. This version is the most efficient of the five.

The fifth version, which was attempted but temporarily set aside, uses a matrix-

free technique. It worked for only the simplest problems. It was probably attempted prematurely, because it needs a very good preconditioner. The diagonal-block preconditioner will, hopefully, allow the matrix-free method to work reliably. The equations for this preconditioner have been worked out in what appears to be an efficient arrangement, but it would have to be programed and tested, and is being left for future work.

The following are several other ideas to improve the implicit code.

1. Set numbers in the Jacobian matrix that are near zero to zero. There would then be fewer elements and perhaps faster convergence, and less memory required.
2. Add damping for greater stability. That is, do not let dY change by more than some fixed percent of Y.
3. Parallelize the code to run on a multiprocessor computer.
4. Optimize settings of the limits and tolerances for a more general set problems. There is some indication that the values for the limits and tolerances need to be changed for different problems, and they are interrelated.
5. Currently the effort has been to try to avoid cutting the time step size at all, which means cutting it in half, but perhaps a smaller decrease in the time-step size would permit a smaller limits on the Newton and Krylov iterations.
6. Explore the possibility that other SPH hydro-forms of the fluid equations might perform better in the implicit code than those being used.

The implicit code may prove useful when used in conjunction with the MLS features being added to SPHINX because MLS is more computationally intensive than standard SPH, as was mentioned in Chapter I Section B. It may help speed up MLS in parts of problems where things are changing very slowly.

There have been a number of unexplained features encountered in the SPHINX code, which, if understood, may help both the implicit and explicit codes. One is the unexplained escaping of particles through the reflecting boundaries. This escape can hap-

pen even when the time-step multiplier is just one. And it has been observed to happen for the explicit code too, but it appears to be a problem only at low velocities. For this reason, the single-jet test case was studied to get away from all reflecting boundaries. This may be an indication of a fundamental problem in the SPH code.

Another problem noted is the occurrence of unexpected elements in the Jacobian when the summation method is used to calculate the density. It is not understood why the explicit code cannot do the rarefaction and shock-tube problems when using the continuity equation. These extra elements in the Jacobian for the summation method may lead to an understanding of why use of the continuity equation does not give the right answer.

Another problem is: when the smoothing length h is allowed to vary, should h be computed before the right-hand-side is computed, or after? If before, it seems to keep h from varying, and if after, h is not consistent with the time derivatives of the rhs() function. The matrix-free method seems to work only if h is consistent with the time derivatives of the right-hand-side computations, but then h does not vary. Where to do the computations for new h's has not been resolved in either the implicit or the explicit code.

The goals of this research have been reached. An implicit code has been written, and it has been shown that it can run a test case with Courant numbers on the order of 3000. It has been shown in several test cases that the accuracy and precision of the code is very good. With more improvements it promises to become a useful working code that can be included as another time-step package for the production code SPHINX.

Appendix

A Rayleigh-Taylor problem with finite boundaries

A derivation of the Rayleigh-Taylor problem with finite boundaries at $z = a$ can be found by starting with the general solution to the equation derived in Hoffman [37], for which he started with the fluid equations and applied perturbation theory and Fourier transformed them and obtained his Eq. (A-27):

$$\frac{\partial}{\partial z}\left(\rho_o \frac{\partial v}{\partial z}\right) = k^2 \rho_o v\left(1 - \frac{g}{\gamma^2 \rho_o}\frac{\partial \rho_o}{\partial z}\right). \tag{A .1}$$

If ρ_o is considered to be constant, Eq. (A .1) reduces to:

$$\frac{\partial^2 v}{\partial z^2} = k^2 v, \tag{A .2}$$

for which the general solution is a sum of exponentials.

$$v(z) = A\, e^{kz} + B\, e^{-kz}. \tag{A .3}$$

The velocity is to vanish at both boundaries and be continuous at the interface. Therefore at $z = +a$, $v(a) = 0$. That is

$$v(a) = A_1 e^{ka} + B_1 e^{-ka} = 0 \quad \text{or} \quad A_1 = -B_1 e^{-2ka}, \tag{A .4}$$

$$\text{thus} \quad v(z>0) = B_1 (e^{-kz} - e^{-2ka} e^{kz}). \tag{A .5}$$

Similarly for $z = -a$, $v(-a) = 0$, and

$$v(-a) = A_2 e^{-ka} + B_2 e^{ka} = 0 \quad \text{or} \quad B_2 = -A_2 e^{-2ka}, \tag{A .6}$$

$$\text{thus} \quad v(z<0) = A_2 (e^{kz} - e^{-2ka} e^{-kz}). \tag{A .7}$$

At the interface the velocities are to be continuous, thus for $z = 0$

$$B_1 (1 - e^{-2ka}) = A_2 (1 - e^{-2ka}), \tag{A .8}$$

or $B_1 = A_2 \equiv v_0$, which is the initial velocity of the interface. Therefore, for the Rayleigh-Taylor problem with finite boundaries at $z = a$ Eq. (A .3) becomes:

$$v(z) = \begin{cases} v_0(e^{-kz} - e^{-2ka}e^{kz}), z > 0 \\ v_0(e^{kz} - e^{-2ka}e^{-kz}), z < 0 \end{cases} . \tag{A .9}$$

The growth rate of the Rayleigh-Taylor problem with finite boundaries can be derived by integrating Eq. (A .1) over a small region of z from $-\varepsilon$ to ε that includes the interface, and then letting ε go to zero. It is assumed that the densities above and below the interface are each constant within their respective regions, so that $\rho(z>0) \equiv \rho_{above}$ and $\rho(z<0) \equiv \rho_{below}$. Integrating the left hand side of Eq. (A .1) and using the derivatives of the results of Eq. (A .9) with respect to z, one obtains:

$$\mathbf{I}_1 \equiv \int_{-\varepsilon}^{\varepsilon} \frac{\partial}{\partial z}\left(\rho_0 \frac{\partial v}{\partial z}\right) dz = \rho_0 \frac{\partial v}{\partial z}\Big|_{-\varepsilon}^{\varepsilon} = -k v_0 (\rho_{above} + \rho_{below})(e^{-k\varepsilon} + e^{-2ka}e^{k\varepsilon}) , \tag{A .10}$$

which, in the limit as ε goes to zero, becomes

$$\mathbf{I}_1 = -k v_0 (\rho_{above} + \rho_{below})(1 + e^{-2ka}) \tag{A .11}$$

The integral of the first term of the right hand side of Eq. (A .1) can be split into integrals above and below the interface:

$$\mathbf{I}_2 \equiv \int_{-\varepsilon}^{\varepsilon} k^2 \rho_0 v dz = \int_{0}^{\varepsilon} k^2 \rho_{above} v dz + \int_{-\varepsilon}^{0} k^2 \rho_{below} v dz \tag{A .12}$$

$$\mathbf{I}_2 = \int_{0}^{\varepsilon} k^2 \rho_{above} v_0 (e^{-kz} - e^{-2ka}e^{kz}) dz + \int_{-\varepsilon}^{0} k^2 \rho_{below} v_0 (e^{kz} - e^{-2ka}e^{-kz}) dz \tag{A .13}$$

$$\mathbf{I}_2 = k^2 \mathrm{v}_0 \left[\rho_{above} \left(\frac{1}{-k} e^{-kz} - e^{-2ka} \frac{1}{k} e^{kz} \right) \Big|_0^{\varepsilon} + \rho_{below} \left(\frac{1}{k} e^{kz} - e^{-2ka} \frac{1}{-k} e^{-kz} \right) \Big|_{-\varepsilon}^{0} \right], \quad \text{(A .14)}$$

$$\mathbf{I}_2 = k^2 \mathrm{v}_0 \left[\frac{1}{-k} \rho_{above} \{ (e^{-k\varepsilon} - 1) + e^{-2ka} (e^{k\varepsilon} - 1) \} \right. \quad , \quad \text{(A .15)}$$
$$\left. + \frac{1}{k} \rho_{below} \{ (1 - e^{-k\varepsilon}) + e^{-2ka} (1 - e^{k\varepsilon}) \} \right]$$

which, in the limit as ε goes to zero, becomes

$$\mathbf{I}_2 = 0. \quad \text{(A .16)}$$

Integrating the last term of the right hand side can be done using integration by parts, and the remaining integral being split up into parts above and below the interface.

$$\mathbf{I}_3 \equiv -\int_{-\varepsilon}^{\varepsilon} k^2 \mathrm{v} \frac{g}{\gamma^2} \frac{\partial \rho_0}{\partial z} dz = -k^2 \frac{g}{\gamma^2} \left[\rho_0 \mathrm{v} \Big|_{-\varepsilon}^{\varepsilon} + \int_{-\varepsilon}^{\varepsilon} \rho_0 \frac{\partial \mathrm{v}}{\partial z} \, dz \right], \quad \text{(A .17)}$$

$$\mathbf{I}_3 = -k^2 \frac{g}{\gamma^2} \left[\rho_0 \mathrm{v} \Big|_{-\varepsilon}^{\varepsilon} + \int_0^{\varepsilon} \rho_{above} \partial \mathrm{v} + \int_{-\varepsilon}^{0} \rho_{below} \partial \mathrm{v} \right], \quad \text{(A .18)}$$

$$\mathbf{I}_3 = -k^2 \frac{g}{\gamma^2} [\rho_{above} \mathrm{v}_0 (e^{-k\varepsilon} - e^{-2ka} e^{k\varepsilon}) - \rho_{below} \mathrm{v}_0 (e^{k\varepsilon} - e^{-2ka} e^{-k\varepsilon}) \quad , \quad \text{(A .19)}$$
$$+ \rho_{above} \mathrm{v}_0 \{ (e^{-k\varepsilon} - 1) - e^{-2ka} (e^{k\varepsilon} - 1) \}$$
$$+ \rho_{below} \mathrm{v}_0 \{ (1 - e^{-k\varepsilon}) - e^{-2ka} (1 - e^{k\varepsilon}) \}]$$

which, in the limit as ε goes to zero, becomes

$$\mathbf{I}_3 = -k^2 \frac{g}{\gamma^2} \mathrm{v}_0 [(\rho_{above} - \rho_{below}) (1 - e^{-2ka})]. \quad \text{(A .20)}$$

From $\mathbf{I}_1 = \mathbf{I}_2 + \mathbf{I}_3$ and Eqs. (A .11), (A .16), and (A .20) the following is obtained:

$$\gamma^2 = k g \frac{(\rho_{above} - \rho_{below})}{(\rho_{above} + \rho_{below})} \frac{(1 - e^{-2ka})}{(1 + e^{-2ka})} . \quad \text{(A .21)}$$

The new part of the result is the ratio of the exponential function. A plot of the function $F = [(1 - e^{-2ka})/(1 + e^{-2ka})]^{1/2}$ shows that for $a = \lambda$ the new function F is equal to approximately one (F = 0.999997), hence does not affect the growth rate, and therefore behaves the same as for the Rayleigh-Taylor problem with infinite boundaries. Not until a is below about $\lambda/2$ does it start to affect the growth rate, and then F = 0.998, which is still a small change. However, it rapidly drops to zero below $\lambda/2$.

References

[6] Arnoldi, W. E. (1951). The Principle of Minimized Iterations in the Solution of the Matrix Eigenvalue Problem, *Quarterly of Applied Mathematics*, **9**, pp. 17-29.

[7] Barrett, R., Berry, M., Chan, T. F., Demmel, J., Donato, J., Dongarra, J., Eijkhout, V., Pozo, R., Romine, C., & van der Vorst, H. (1994). *Templates for the Solution of Linear Systems: Building Blocks for Iterative Methods,* SIAM, Philadelphia.

[8] Barrett, R. (July, 1994). Algorithmic Bombardment for the Iterative Solution of Linear Systems: A Poly-Iterative Approach, Masters thesis, University of Tennessee, Knoxville, Tennessee.

[9] Belytschko, T., Lu, Y. Y., & Gu, L. (1994). Element-Free Galerkin Methods, *Int. J. for Numerical Methods in Engineering*, **37**, pp. 229-256.

[10] Benz, W. (1989). Smooth Particle Hydrodynamics: A Review, *Harvard-Smithsonian Center for Astrophysics*, No. 2884.

[11] Benz, W. & Asphaug, E. (1995). Simulations of Brittle Solids Using Smooth Particle Hydrodynamics, *Computer Physics Communications*, **87**, pp. 253-265.

[12] Cash, J. R. & Psihoyios, Y. (1996). The MOL Solution of Time Dependent Partial Differential Equations, *Computers Math. Applic.*, **31**, No. 11, pp. 69-78.

[13] Chandrasekhar, S. (1981). *Hydrodynamic and Hydromagnetic Stability*, Dover Publications, New York.

[14] Choi, C. K., Hoffman, N. M., Clover, M. R., Powers, W. J. (1997), Simulations of Linear and Nonlinear Rayleigh-Taylor Instability Under High Atwood Numbers, Proceeding of 1997 Laser Interactions and Plasma Phenomena (LIRPP).

[15] Cloutman, L. D. (1991). An Evaluation of Smoothed Particle Hydrodynamics, an article in: *Advances in the Free-Lagrange Method*, Proceedings of the Next Free-Lagrange Conference, Jackson Lake, Moran, Wy., USA, H. E. Trease, M. J. Fritts, W. P. Crowley (Eds.), Lecture Notes in Physics **395**, Springer-Verlag, New York, pp. 229-238.

[16] Coleman, T. F., Garbow, B. S. & More, J. J. (Sept., 1984). Software for Estimating Sparse Jacobian Matrices, *ACM Transactions on Mathematical Software*, **10**, No. 3, pp. 329-345.

[17] Coleman, T. F. & Van Loan, C. (1988). *Handbook for Matrix Computations*, SIAM, Philadelphia.

[18] Crotzer, L. A., Dilts, G. A., Knapp, C. E., Morris, K. D., Swift, R. P., & Wingate, C. A. (April, 1998). SPHINX Manual Version 11.0, Los Alamos National. Lab. Manual: LA-13436-M.

[19] Cullum, J. K. & Willoughby, R. A. (1985). *Lanczos Algorithms for Large Symmetric Eigenvalue Computations Vol. I Theory, (Vol. II Programs)*, Birkhäuser, Boston.

[20] Curtis, A. R., Powell, M. J. D., & Reid, J. K. (1974). On the Estimation of Sparse Jacobian Matrices, *J. of the Inst. of Maths. and it's Applics.*, **13**, pp. 117-119.

[21] Degnan, J. H., Baker, W. L., Cowan, M, Jr., Graham, J. D., Holmes, J. L., Lopez, E. A., Price, D. W., Ralph, D., & Roderick, N. F. (May, 1999). Operation of Cylindrical Array of Plasma Guns, *Fusion Technology*, **35**, pp.354-360.

[22] Dilts, G. A. (1997). Moving-Least-Squares-Particle Hydrodynamics I Consistency and Stability, Los Alamos National. Lab. Report: LA-UR-97-4168.

[23] Dilts, G. A. (1998). Conservative Moving-Least-Squares Methods for Lagrangian Hydrodynamics, Los Alamos National. Lab. Report: LA-UR-98-304.

[24] Duff, I. S. & Reid, J. K. (June, 1978). An Implementation of Tarjan's Algorithm for the Block Triangularization of a Matrix, *ACM Transactions on Mathematical Software,* **4**, No. 2, pp. 137-147.

[25] Dukowicz, J. K. & Meltz, B. J. A. (1991). Vorticity Errors in Multidimensional Lagrangian Codes, an article in: *Advances in the Free-Lagrange Method*, Proceedings of the Next Free-Lagrange Conference, Jackson Lake, Moran, WY., H. E. Trease, M. J. Fritts, W. P. Crowley (Eds.), Lecture Notes in Physics 395, Springer-Verlag, New York, pp. 289-292.

[26] Freund, R. W. & Nachtigal, N. M. (1991). QMR: a Quasi-Minimal Residual Method for Non-Hermitian Linear Systems, *Numerische Mathematik*, **60**, pp. 315-339.

[27] Fulk, D. A. (1994). A Numerical Analysis of Smoothed Particle Hydrodynamics, Ph.D dissertation, Dept. of Mathematics and Statistics, Air Force Institute of Technology, Wright Patterson AFB, Ohio.

[28] Fulk, D. A. & Quinn, D. W. (1996). An Analysis of 1-D Smoothed Particle Hydrodynamics Kernels, *Journal of Computational Physics*, **126**, No. 1, pp. 165-180.

[29] Gear, G. W. (1971). *Numerical Initial Value Problems in Ordinary Differential Equations*, Prentice-Hall Inc., Englewood Cliffs, New Jersey.

[30] Gingold, R. A. & Monaghan, J. J. (1977). Smoothed Particle Hydrodynamics: Theory and Application to Non-Spherical Stars, *Mon. Not. Roy. Astron. Soc.* **181**, pp. 375-389.

[31] Goldston, R. J. & Rutherford, P. H. (1995), *Introduction to Plasma Physics*, Institute of Physics Publishing, Bristol and Philadelphia.

[32] Golub, G. H. & Van Loan, C. F. (1996). *Matrix Computations*, 3rd Ed., The Johns Hopkins University Press, Baltimore, (Note: the 1st and 2nd Eds. do not cover iterative methods for non-symmetric linear systems).

[33] Graham, M. J. (1996). A Numerical Study of the Richtmyer-Meshkov Instability in Cylindrical Geometry, a Ph.D. dissertation for the Dept. of Applied Mathematics and Statistics from the State University of New York.

[34] Hernquist, L. & Katz, N. (June, 1989). TREESPH: A Unification of SPH with the Hierarchical Tree Method, *The Astrophysical Journal Supplement Series,* **70**, pp. 419-446.

[35] Hestenes, M. R. & Stiefel, E. L. (1952). Methods of Conjugate Gradients for Solving Linear Systems, *J. of Research of the National Bureau of Standards*, Section B, **49**, pp. 409-436.

[36] Hockney, R. W. & Eastwood, J. W. (1988). Computer Simulation Using Particles, Adam Hilger, Bristol.

[37] Hoffman, N. M. (1995). "Hydrodynamic Instabilities in Inertial Confinement Fusion," *Laser Plasma Interactions 5: Inertial Containment Fusion*, Hooper, M. B., ed., Institute of Physics Publishing, Bristol, pp. 105-137.

[38] Householder, A. S. (1964). *Theory of Matrices in Numerical Analysis*, Dover Publications, New York.

[39] Johnson, G. R. (1996). Artificial Viscosity Effects for SPH Impact Computations, *Int. J. Impact Engineering.*, **18**, No. 5, pp. 477-488.

[40] Kaps, P. & Rentrop, P. (1979). Generalized Runge-Kutta Methods of Order Four with Stepsize Control for Stiff Ordinary Differential Equations, *Numer. Math.*, **33**, pp. 55-68.

[41] Kelley, C. T. (1995). *Iterative Methods for Linear and Nonlinear Equations*, SIAM, Philadelphia.

[42] Kirkpatrick, R. C,. & Lindemuth, I. R, (1997) Magnetized Target Fusion, An Overview of the Concept, *Current Trends in International Research*, ed. E. Panarella, Plenum Press, New York.

[43] Knoll, D. A., Rider, W. J., & Olson, G. L. (1998). An Efficient Nonlinear Solution Method for Nonequilibrium Radiation Diffusion, Los Alamos National. Lab. Report: LA-UR-98-2154. Also submitted for publication to: *J. of Quantitative Spectroscopy and Radiative Transfer.*

[44] Kopal, Z. (1961). *Numerical Analysis*, 2nd Ed., John Wiley & Sons Inc., New York.

[45] Lanczos, C. (1950). An Iteration Method for the Solution of the Eigenvalue Problem of Linear Differential and Integral Operators, *J. of Research of the National Bureau of Standards,* **45**, pp. 255-482.

[46] Landau, L. D. & Lifshitz, E. M. (1975). *Fluid Mechanics*, Pergamon Press, Oxford.

[47] Lanczos, C. (1952). Solution of Systems of Linear Equations by Minimized Iterations, *J. of Research of the National Bureau of Standards,* **49**, pp. 33-53.

[48] Libersky, L. D. & Petschek, A. G. (1991). Smooth Particle Hydrodynamics with Strength of Materials, an article in: *Advances in the Free-Lagrange Method*, Proceedings of the Next Free-Lagrange Conference, Jackson Lake, Moran, Wy., USA, H. E. Trease, M. J. Fritts, W. P. Crowley (Eds.), Lecture Notes in Physics 395, Springer-Verlag, New York, pp. 248-257.

[49] Libersky, L. D. & Randles, P. W. (1998). Boundary Conditions in a Meshless Staggered Particle Code, Los Alamos National. Lab. Report: LA-UR-98-590.

[50] Lindemuth, I. R., & Kirkpatrick, R. C. (1991). The Promise of Magnetized Fuel: High Gain in Inertial Confinement Fusion, *Fusion Technology*, **20**, pp. 829-833. Also a Los Alamos National. Lab. Report: LA-UR-91-2498.

[51] Lucy, L. (1977). A Numerical Approach to Testing the Fission Hypothesis, *Astron, J.*, **82**, pp. 1013-1024.

[52] Mandell, D. A., Wingate, C. A., Dilts, G. A., Schwalbe, L. A. (Oct. 1996). Computational Brittle Fracture Using Smooth Particle Hydrodynamics (U), Los Alamos National. Lab. Report: LA-CP-96-209.

[53] Martin, J. C. & Moyce, W. J. (1952) Part IV. An Experimental Study of the Collapse of Liquid Columns on a Rigid Horizontal Pane, *Phil. Trans. of the Royal Soc. of London*, **244**, pp. 312-324.

[54] Mendelson, A. (1970). *Plasticity: Theory and Application*, The Macmillan Co., New York, New York. Reprinted in 1991 by University Microfilms International (UMI) Out-of-Print Books on Demand, Ann Arbor, Michigan.

[55] McCormick, S. T. (1983). Optimal Approximation of Sparse Hessians and its Equivalence to a Graph Coloring Problem, *Mathematical Programming*, **26**, pp. 153-171.

[56] Monaghan, J. J. (1982). Why Particle Methods Work, *SIAM J. on Scientific and Statistical Computing*, **3**, No. 4, pp. 422-433.

[57] Monaghan, J. J. (1985). A Refined Particle Method for Astrophysical Problems, *Astronomy and Astrophysics*, **149**, pp. 135-143.

[58] Monaghan, J. J. (1985). Particle Methods for Hydrodynamics, *Computer Physics Reports*, **3**, pp. 71-124, (North-Holland, Amsterdam).

[59] Monaghan, J. J. (1988). An Introduction to SPH, *Computer Physics Communications,* **48**, pp. 89-96, (North-Holland, Amsterdam).

[60] Monaghan, J. J. (1992). Smoothed Particle Hydrodynamics, *Annual Review of Astronomy and Astrophysics*, **30**, pp. 543-574.

[61] Monaghan, J. J. (1994). Simulating Free Surface Flows with SPH, *Journal of Computational Physics*, **110**, pp. 399-406.

[62] Monaghan, J. J. & Gingold, R. A (1983). Shock Simulation by the Particle Method SPH, *Journal of Computational Physics*, **52**, pp. 347-389.

[63] Mousseau, V. A. (May, 1996). Fully Implicit Kinetic Modelling of Collisional Plasmas, a Ph. D. dissertation from the University of Idaho, also report number INEL-96/ 0149 Idaho National Engineering Laboratory.

[64] Oran, E. S. & Boris, J. P.(1987). *Numerical Simulation of Reactive Flow*, Elsevier Science Publishing Co. Inc., New York.

[65] Press, W. H. & Teukolsky, S. A. (May/June 1989). Integrating Stiff Ordinary Differential Equations, *Computers in Physics*, pp. 88-91.

[66] Press, W. H., Teukolsky, S. A., Vetterling, W. T., & Flannery, B. P. (1995). *Numerical Recipes in C the Art of Scientific Computing, 2nd Ed.*, and *Numerical Recipes Example Book [C], 2nd Ed*, Cambridge University Press, Cambridge.

[67] Pritchett, J. W. & Rice, M. H. (1975). User's Guide to the AQUA Subprogram System - A Comprehensive Constitutive Package for Water, S-Cubed Report: SSS-IR-75-2544.

[68] Rice, M. H., Gurtman, G. A., & Skoller, B. (1997). SPHINX Code Enhancements Appropriate to Tactical Missile Defense Engagements, DSWA-TR-97-35.

[69] Rider, W. J. (1993). Stability of Semi- and Nearly-Implicit Schemes for Thermal-Hydraulics, presented at the National Heat Transfer Conference 1993.

[70] Rosenbrock, H. H. (1963). Some General Implicit Processes for the Numerical Solution of Differential Equations, *Computer Journal*, **5**, pp. 329-330.

[71] Saad, Y. (1996). *Iterative Methods for Sparse Linear Systems*, PWS Publishing Company, Boston.

[72] Saad, Y. & Schultz, M. H. (1986). GMRES: A Generalized Minimal Residual Algorithm for Solving Nonsymmetric Linear Systems, *SIAM J. on Scientific and Statistical Computing*, **7**, pp. 856-869.

[73] Serna, A., Alimi, J. M., & Chieze, J. P. (1996). Adaptive Smooth Particle Hydrodynamics and Particle-Particle Coupled Codes: Energy and Entropy Conservation, *Astrophysical Journal*, **461**, No. 2, pt. 1, pp. 884-896.

[74] Siemon, R. E., Lindemuth, I. R., & Schoenberg, K. F. (Dec. 1997). Why Magnetized Target Fusion Offers A Low-Cost Development Path for Fusion Energy, *Comments on Plasma Physics and Controlled Fusion.*

[75] Sonneveld, P. (1989). CGS, a Fast Lanczos-Type Solver for Nonsymmetric Linear Systems, *SIAM J. on Scientific and Statistical Computing*, **10**, No. 1, pp. 36-52.

[76] Stellingwerf, R. F., Buff, J. (April, 1978). Stability of Astrophysical Gas Flow. I. Isothermal Accretion, *The Astrophysical Journal*, **221**, pp. 661-671.

[77] Stellingwerf, R. F. (August, 1983). HYDRA: An Implicit Partial Differential Equation, Relaxation, Stability Analysis Package, *The Astrophysical Journal*, **271**, pp. 876-878.

[78] Stellingwerf, R. F. (1991). Smooth Particle Hydrodynamics, an article in: *Advances in the Free-Lagrange Method*, Proceedings of the Next Free-Lagrange Conference, Jackson Lake, Moran, Wy., USA, H. E. Trease, M. J. Fritts, W. P. Crowley (Eds.), Lecture Notes in Physics 395, Springer-Verlag, New York, pp. 239-247.

[79] Stellingwerf, R. F. & Wingate, C. A. (1992). Impact Modeling With Smooth Particle Hydrodynamics, (submitted to the 1992 Hypervelocity Impact Symposium, November17-20, 1992), Los Alamos National. Lab. Report: LA-UR-92-1981.

[80] Stoer, J. & Bulirsch, R., English Translation: (1980). *Introduction to Numerical Analysis*, Springer-Verlag Inc., New York.

[81] Strang, G. (1986). *Introduction to Applied Mathematics*, Wellesley-Cambridge Press, Wellesley, Mass.

[82] Swegle, J. W., Hicks, D. L., & Attaway, S. W. (1993). Smoothed Particle Hydrodynamics Stability Analysis, *J. of Computational Physics*, **116**, pp. 123-134.

[83] Swift, R. P., Hagelberg, C. R., Carney, T. C., Greening, D., Hiltl, M. (Feb. 14-17, 2000). Modeling Stress-Induced Damage from Impact Recovery Experiments, Proceedings of the ETCE/OMAE 2000 Joint Conference: Energy for the New Millennium, New Orleans, La.

[84] Thio, Y. C. F., Knapp, C. E., & Kirkpatrick, R. C. (1998). The Feasibility of Merged Compact Toroids Compressed By Multiple Plasma Jets as a Possible Embodiment of MTF, a poster presented at the 1998 Innovative Confinement Concepts Workshop, at Princeton, NJ, April 6-9 1998.

[85] Thio, Y. C. F., Kirkpatrick, R. C., Knapp, C. E., Panarella, E., Wysocki, F. J., & Parks, P. (1998). An Embodiment of Magnetized Target Fusion in a Spherical Geometry with Stand-off Drivers, a Los Alamos Natl. Lab. Report: LA-UR-98-269. Also presented at the 1998 Innovative Confinement Concepts Workshop, at Princeton, NJ, April 6-9 1998. Also presented at the ICOPS '98, Raleigh, NC, June 1-4, 1998. Also to be published in *Current Trends in International Fusion Research - Proceedings of the Second Symposium*, E. Panarella (ed.), National Research Council of Canada Press, 1999.

[86] Timmes, F. X. (1993). Reactive Flows in Compact Objects, Ph.D dissertation, Dept. of Astronomy and Astrophysics, University of California, Santa Cruz.

[87] Warren, M. S. & Salmon, J. K. (1995). A Portable Parallel Particle Program, *Computer Physics Communications*, **87**, pp. 266-290.

[88] Weaver, T. A., Zimmerman, G. B., & Woosley, S. E. (Nov. 1, 1978). Presupernova Evolution of Massive Stars, *The Astrophysical Journal*, **225**, pp. 1021-1029.

[89] Wells, D. R., Ziajka, P. E., & Tunstall, J. L. (1986). Hydrodynamic Confinement of Thermonuclear Plasmas Trisops VIII (Plasma Liner Confinement), *Fusion Technology*, **9**, pp. 83-96.

[90] Wendroff, B. (1966). *Theoretical Numerical Analysis*, Academic Press Inc., New York.

[91] Wendroff, B. (1969). *First Principles of Numerical Analysis*, Addison Wesley Publishing Co., Reading, Massachusetts.

[92] Wingate, C. A., Dilts, G. A., Mandell, D. A, Crotzer, L. A., Knapp, C. E., & Libersky, L. D. (1998). Progress in Smooth Particle Hydrodynamics, (submitted to the Fourth World Congress on Computational Mechanics, Buenos Aires, Argentina, June 29 - July 2, 1998) Los Alamos National. Lab. Report: LA-UR-98-582.

[93] Wingate, C. A., Stellingwerf, R. F., Davidson, R. F., & Burkett, M. W. (1992). Models of High Velocity Impact Phenomena, (submitted to the 1992 Hypervelocity Impact Symposium, November17-20, 1992), Los Alamos National. Lab. Report: LA-UR-92-1982.

[94] Wingate, C. A. & Stellingwerf, R. F. (1993). Smooth Particle Hydrodynamics - The SPHINX and SPHC Codes (submitted to the 1993 ASME Winter Meeting, November 28 - December 4, 1993), Los Alamos National. Lab. Report: LA-UR-93-1938.

[95] Wingate, C. A. & Stellingwerf, R. F. (1995). Los Alamos SPHINX Manual Version 7.6, Los Alamos National. Lab. Report: LA-UR-93-2476

[96] Zel'dovich, Ya. B. & Raizer, Yu. P. (1967). Physics of Shock Waves and High-Temperature Hydrodynamic Phenomena, Volumes I & II, Academic Press, New York.

[97] Zlatev, Z. (1991). *Computational Methods for General Sparse Matrices*, Kluwer Academic Publishers, Boston.

ACKNOWLEDGEMENTS

I wish to acknowledge and thank the people who made this dissertation possible. My advisor at the University of New Mexico (UNM) Chemical and Nuclear Engineering (ChNE), Dr. Norman F. Roderick, and my advisor at the Los Alamos National Labs (LANL), Dr. Charles A. Wingate have both contributed immensely to my learning and understanding of the broad range of subjects needed to conduct this research. In addition to my two advisors, I also want to thank the others on my committee: Dr. Deborah L. Sulsky (Mathematics and Statistics, UNM); Dr. Anil K. Prinja (ChNE, UNM); and Dr. Gary W. Cooper (ChNE, UNM). I also want to acknowledge the significant technical consultation given by the following people (alphabetically): Dr. Daniel C. Barnes, Dr. Richard F. Barrett, Dr. Michael R. Clover, Dr. Stephen V. Coggeshall, Dr. Charles W. Cranfill, Dr. Gary A. Dilts, Dr. Doran R. Greening, Dr. Nelson M. Hoffman, Dr. Ronald C. Kirkpatrick, Dr. Dana A. Knoll, Dr. William D. Nystrom, Dr. William J. Rider, Dr. Peter T. Sheehey, Dr. D. Palmer Smitherman, Dr. Robert F. Stellingwerf, Dr. Y. C. Francis Thio, and Dr. Robert B. Webster. I also thank the group leaders at LANL who have supported me financially in doing this work: Dr. Douglas C. Wilson, Dr. Robert C. Little, and Dr. Len G. Margolin. Thank you all.

Los Alamos
NATIONAL LABORATORY
Los Alamos, New Mexico 87545